Fracture detection using PS converted waves – A case study from Daqing oil field

Hengchang Dai, and Xiang-Yang Li, British Geological Survey; Richard Ford, Imperil College London; Chenye Yu, PetroChina Daqing Oilfield Limited; Jianmin Wang, CNPC Daqing Geophysical Exploration*

Summary

We performed a case study to use PS converted waves for fracture detection for a 3D land dataset. In this study, the azimuthal variation of NMO velocity of PS converted waves is used to detect the fracture properties. The direction of maximum velocity indicates the fracture direction and the velocity perturbation indicates the anisotropy. The stack image when compensated for azimuthal velocity variation showed enhancements in terms of reflection and fault definition. The mapped distribution of the direction of maximum velocity and the velocity perturbation outlined the fracture system of the reservoir and showed a clear trend between the direction of maximum velocity and the Daqing anticline location.

Introduction

In recent years multi-component 3D seismic data have demonstrated their usefulness for characterising fractured reservoirs. In fractured reservoirs, fractures are generally aligned in a preferred direction which depends on the stress history, and this often gives rise to horizontal transverse isotropy (or HTI). Knowing the direction of fractures as *a priori* information before drilling is especially useful for the placement of horizontal or deviated wells. Many theoretical and field studies have shown that the azimuthal variation in wavefield attributes (such as velocity and amplitude) can be used for fracture detection (Tsvankin, 1997, Li *et al.,* 2003, Vetri *et al.,* 2003; and Zhu *et al.,* 2008, Qian *et al.,* 2008).

The azimuthal variation of NMO velocities and moveout is one of the most useful attributes for detecting natural fractures. Tsvankin (1997) proved that the NMO velocity of single mode waves (P and S wave) in HTI media is an ellipse in the azimuthal plane, and its major axis is the direction of fracture strike. Based on this, many applications have been developed to use the azimuthal variation of P-wave NMO velocity to detect and assess natural fractures. A PS converted wave is a combination of P and S waves and takes the behaviour of P and S waves. The NMO velocity and moveout of PS converted waves also have a similar azimuthal variation and can be used for fracture detection. In this paper, we shows an example from Daqing oil field, China, which uses the PS converted waves to detect the fractures.

Azimuthal variation of the velocity and moveout of PS converted waves.

In 3D data processing, azimuthal anisotropy can be observed in the common-offset-common-azimuth cube (Zhu, 2008). After NMO correction, the residual NMO anomalies vary with azimuthal direction. This variation is normally represented as a cosine function. For PS converted waves, the NMO is controlled by the velocity model which includes four parameters: V_{ps}, γ_0, γ_{eff}, and χ_{eff} (Li and Yuan, 2003). The azimuthal variation in any of the four parameters may contribute to the azimuthal variation in residual NMO anomalies. However the four parameters have different sensitivities to PS wave moveout. The PS wave velocity V_{ps} is most sensitive. For weak anisotropy, the azimuthal variation in γ_0, γ_{eff}, and χ_{eff} can be neglected and only the azimuthal variation in V_{ps} considered. Note that here the PS wave is referred to as the PS converted-wave recorded in the radial component. According to the azimuthal variation of residual NMO anomalies, the azimuthal variation in PS wave velocity can be written as:

$$V_{ps}(\theta) = V_0[1+\alpha\cos 2(\theta-\beta)] \qquad (1)$$

where V_0 is the base velocity, α the velocity perturbation, and β the direction of maximum velocity (e.g. the fracture direction), and θ the ray path azimuth. The PS converted wave moveout can then be written as:

$$t_{ps}^2 = t_{ps0}^2 + \frac{h^2}{V_{ps}^2(\theta)} - \frac{2\kappa h^4}{V_{ps}^2(\theta)[t_0^2 V_{ps}^2(\theta) + m\cdot h^2]}\,. \qquad (2)$$

Where κ and m are functions of γ_0, γ_{eff}, and χ_{eff}. This moveout is used to perform the NMO correction in 3D PS converted wave data processing.

Processing flow

Based on equations 1 and 2, we have developed an approach and developed necessary tools (Dai and Li 2010). Figure 1 shows the processing flow of this approach to estimate the azimuthal variation of the PS wave velocity and compensate for the azimuth anisotropy. The PS wave data are firstly sorted into ACP gathers. For estimating the azimuthal variation of PS wave velocity, ACP gathers have to be combined into super gathers to increased the trace fold and enhance the signal-to-noise ratio. Each ACP super-gather will be divided into azimuthal sub-gathers according to azimuth. For each azimuthal sub-gather, velocity analysis is applied to estimate the azimuthal velocities. A least-square fitting technique is used to fit these estimated velocities in equation 1. V_0 , α and β obtained from this fitting show the azimuthal anisotropy and fracture properties and also can be used to compensate for the effect of azimuthal anisotropy in NMO correction to enhance image quality.

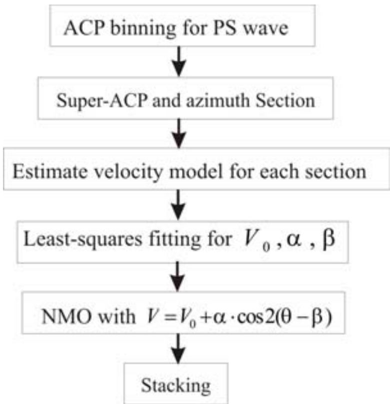

Figure 1. Processing flow for compensating azimuth anisotropy

3D-3C data from Daqing oilfield

The Daqing oilfield within the Songliao Basin is located in Heilongjiang province, NE China. 3D seismic acquisition was performed in 2005 directly in the region where hydrocarbon production had been occurring for 30 years. The 3D survey area is 18.85 km ESE-WNW and 6.4 km in a NNE-SSW trending direction. 3-Component (3C) geophones were used with the sole purpose of extending previous methods of characterising the reservoir by processing PS converted waves. Two swathes of the 3D dataset are used in this study. Figure 2 shows the location of the two swath dataset.

The Songliao Basin is defined as a Cretaceous rift depression basin (Desheng, 1995) located in a complicated tectonic region between the North China and Siberian plates. The large-scale tectonic regime was N-S in the Early Mesozoic driven by the interaction of these two plates. The tectonic setting changed with the assembly of the European-Asian continent in the Late Mesozoic and has since become part of the aforementioned active China belt. A series NE-NNE trending faults now characterise the orientation of the tectonic belt, which encompasses the Songliao, West Liaoning, and North Liaoning Basins (Jishun & Liwei, 2002).

There are many reservoir rock types in the Songliao Basin, as during the extensional tectonic phase (stage II) rapid subsidence created accommodation space for alluvial fan deposits, which formed concentric distributions of facies around lacustrine regions throughout the basin. This led to reservoir intervals in the subsurface above, below, and laterally adjacent to the prolific source rocks. This scenario typifies highly favourable conditions for hydrocarbon migration. Other reservoir intervals include flood and delta plain facies delta front / shallow lake facies, and near-shore silt facies (Desheng, 1995). Traps within the basin were created in the final stage of the tectonic evolution and are dominated by regional-scale domal anticlines interspersed with synclines. The Daqing oilfield lies at the centre of the Songliao basin in one of these domed anticlines. Figure 3 show the cross section of the Songlian Basin.

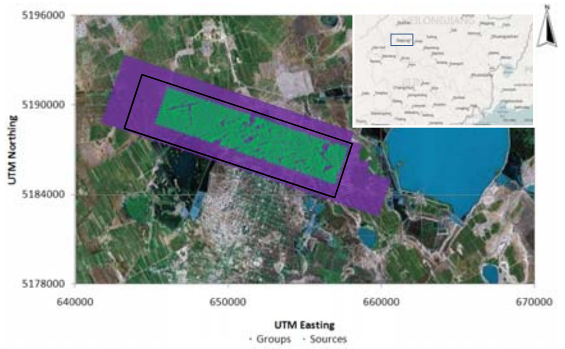

Figure 2. The geometry of 3D acquisition in the Daqing oilfield. The green markers show locations of dynamite sources and purple points indicate receiver locations.

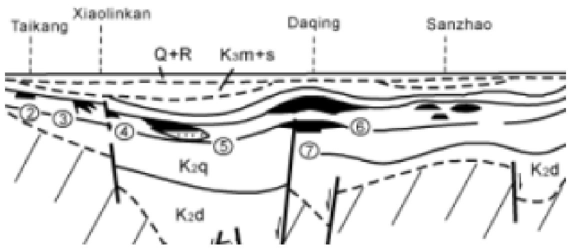

Figure 3. Cross section of the Songliao Basin showing the main reservoirs. After Jishun and Liwei (2002).

Processing results and discussions

After binning the data into ACP gathers, a 3D grid of super-gathers were created by using 20 adjacent ACP gathers in the inline direction and 20 adjacent ACP gathers in the crossline direction. There are sufficient ACP binned traces in the super-gather for multi-azimuth analysis. There are 8 super-gather lines and each super-gather line comprises of 17 super-gathers. In each super-gather, traces are separated according to azimuthal direction and binned into 6 sections with azimuthal binning size of 30^o. Velocity analysis was performed for these azimuthal super-gathers. For each super-gather, 6 velocity profiles are estimated and then used to calculate the azimuthal velocity parameters. Figure 4 shows an example of the velocity analysis. In the velocity analysis, the NMO correction is applied using the same velocity model. In Figure 4a, the events are under-corrected; in Figure 4b, the events are over-corrected. In order to flatten the events, the velocity should be reduced in Figure 5a and increased in Figure 4b. This shows the azimuthal variations of the NMO velocity.

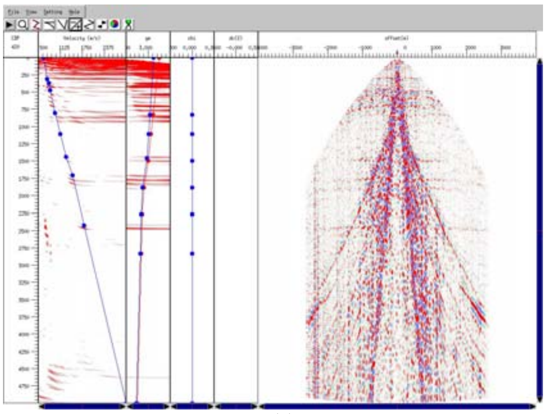

(a)

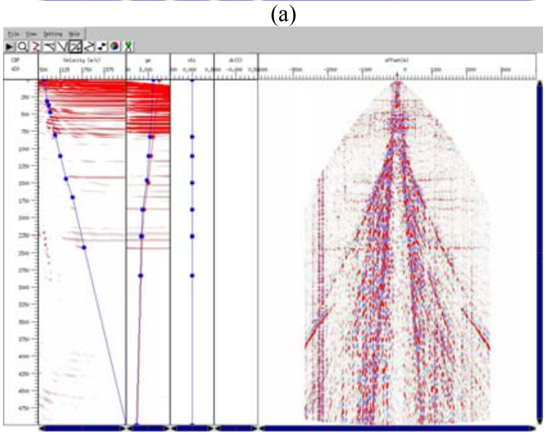

(b)

Figure 4. Examples of velocity analysis of azimuthal super gathers. (a) Azimuth of -60º - -30º and (b) azimuth of 30º - 60º.

To compensate for the effects of the azimuthal anisotropy, the NMO correction uses the velocity calculated according to the trace azimuth. Figure 5 shows the stacked image which uses azimuthal velocity. For comparison, Figure 6 shows the stacked image which uses the base velocity. The two images are similar but Figure 5 shows subtle improvement where azimuthal velocity is applied. The majority of improvements occur at the peak of the anticline at 1.5 seconds between CDP 350 and 450; smaller changes are also observed at the 2.5 second reflection event. For example, in compensating for azimuthal velocity variations, the reflected event which corresponds to large velocity perturbations (Figure 7) shows stronger energy.

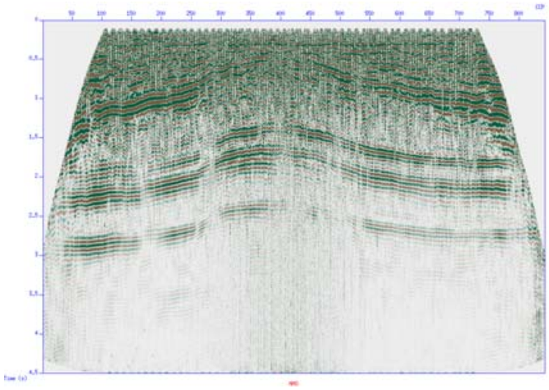

Figure 5. Stacked image of CDP line 400 with azimuthal variation in NMO velocity.

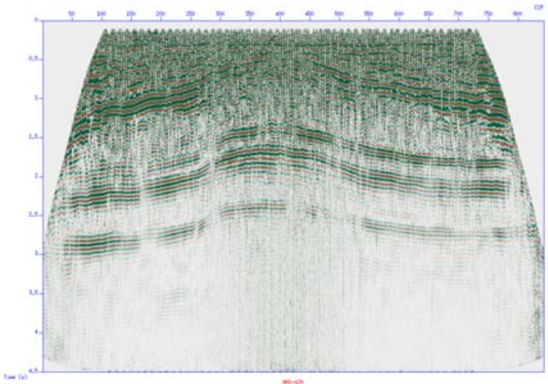

Figure 6 Stacked image of CDP line 400 without azimuthal variation

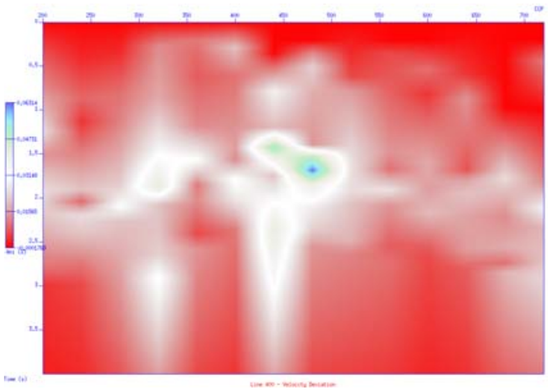

Figure 7. Velocity perturbation of CDP line 400

The distribution map of azimuthal velocity can provide a tool to indicate the fracture parameters. This map is created by plotting the direction of the maximum velocity angle in a time slice for a given horizon. Figure 8 shows three time-slices at 1.5s, 1.8s, and 2.4s.

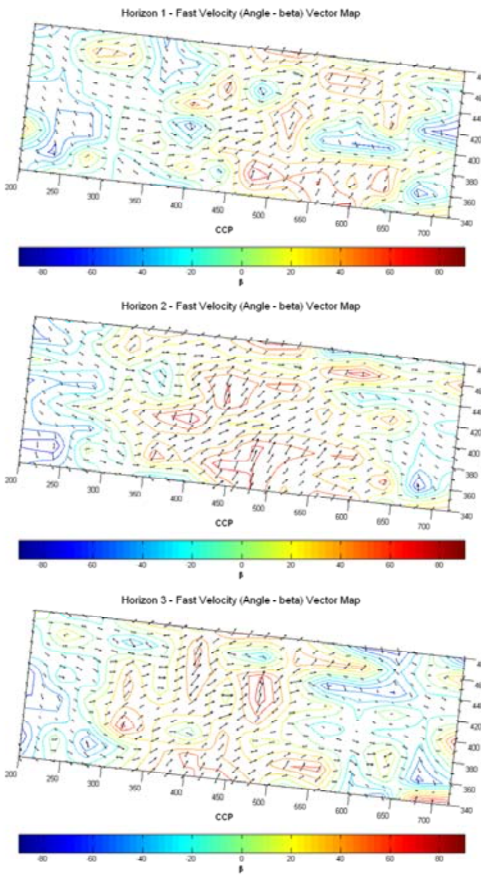

Figure 8. Time-slices show the distribution map of β for horizons 1-3 at the time 1.5s, 1.8s and 2.3s. Arrows are superimposed on the contour map for guidance. The size of the arrow represents α . The axes are rotated in accordance with the inline / crossline orientation (see Figure 1). 0° represents the inline direction.

The time slices for these horizons can provide information on the fracture density and direction. We found that a consistent trend of ENE to NE oriented fractures lie in the region at the centre of the anticline (between CDPs 420-480 and lines 380 – 420). In this location, there is also an increase in the fracture density. The nature of anisotropy was asymmetrical for the three analysed horizons, with locations for regions of high-fracture density migrating laterally with depth. The interpreted migration could also be attributed to isolated locations of high-fracture density. However, superimposing the results onto line 440 showed that there is a region associated with a decrease in image resolution associated with the fracture swarms. The fracture orientation was poorly defined although the trend was found to be close to the direction of maximum horizontal compressional stress. The sharp changes in velocity perturbation are indicative of faults or fracture swarms in the anticline. An interpreted fault was found to be trending NW-SE, almost perpendicular to the strike of the Songliao basin. Linking this fault to seismic stacks was difficult, as there was a lack of consistency between the velocity perturbation and the stacked images.

For each individual horizon there is a clear trend between increases of β and the Daqing anticline location. However, defining a relationship between β and the anticline position is not as clear as for calculations of α . There is an apparent depth-related trend in which high values of β (or fracture orientations to the north and east) migrate westwards. This is also observed by α between lines 400 and 480 close to ACP 400. Values of β outside the anticline region trend NW-SE, these regions are also regions of low α . Fitting of the velocity-ellipse for low α will yield poor values for β, and therefore with a low fracture density it is difficult to determine if the direction of fracture strike is accurate. The relationship now shows that in regions where there is high α , the dominant fracture orientation is approximately NE-SW. There is some variation in the NE-SW trend, with horizon 2 exhibiting close to a northward fracture strike corresponding to the highest α values for that horizon.

Conclusions

In this study, we use the azimuthal variation of NMO velocity of PS converted waves to detect fracture properties. The processing results from the 3D land data show that azimuthal variation of NMO velocity of PS converted wave is a useful tool to describe the fracture system in the reservoir. The distribution map of the maximum velocity direction and the velocity perturbation shows a clear trend between the direction of maximum velocity and the Daqing anticline location. The stack image compensated for azimuthal velocity variation showed enhancements in terms of reflection and fault definition.

Acknowledgements

We thank Daqing Oil Field of China for providing the 3D datasets. This work is supported by the Edinburgh Anisotropy Project (EAP) of the British Geological Survey, and is published with the permission of the Executive Director of the British Geological Survey (NERC) and the EAP sponsors.